Modelling the degradation of acidic and alkaline printing paper

J. Tétreault, D. Vedoy, P. Bégin, S. Paris Lacombe, Anne-Laurence Dupont

Modelling the degradation of acidic and alkaline printing paper

J. Tétreault[1], D. Vedoy[1], P. Bégin[1], S. Paris Lacombe[2], A.-L. Dupont*[2]

[1] *Canadian Heritage, Canadian Conservation Institute, 1030 Innes road, Ottawa, ON K1B4S7, Canada*

[2] *Centre de Recherche sur la Conservation, CNRS, Muséum National d'Histoire Naturelle, 36 rue Geoffroy St Hilaire, 75005 Paris, France*

***Corresponding author:** anne-laurence.dupont@mnhn.fr*

Abstract There has always been an interest in the professional communities of libraries, archives and conservation science to find ways of estimating the rate of degradation of paper under archival conservation conditions. Previously we reported a number of considerations for developing a kinetic degradation model based on Whatman no.1 paper. In the present research, this model was extended to 10 different papers and validated. Various physical and chemical properties of acidic, neutral, and alkaline papers were measured, such as the degree of polymerization (DP), tensile strength, equilibrium moisture content (EMC), and pH, as well as alkaline fillers content when applicable. The activation energy (E_a) based on DP of cellulose and zero-span tensile strength were determined. E_a and pH had the most significant influence on the simulated decay of paper. Papers with a high E_a (> 120 kJ mol^{-1}), alkaline such as those containing at least 2% $CaCO_3$, and acidic –but good printing quality papers made of bleached chemical pulp– were found the most durable in ambient conditions. Papers with a lower E_a (< 110 kJ mol^{-1}) such as lignocellulosic papers containing significant amount of mechanical pulp were much less stable over time. Whatman filter papers, used as models of pure cellulosic papers, were found to have low E_a despite the good quality cotton fibers. A generic isoperm equation based on E_a was developed to predict the changes in the state of papers under various climatic conditions, and was applicable independently of the pH of the paper. The model developed allows a better quantification of the deterioration rate of printing papers such as those that are currently, and will be in the future, found in our archival collections.

Keywords Cellulose · Degradation · Hydrolysis · Environment · Modelling · Degree of polymerization

Introduction

In the mid-nineteenth century, papermaking technology underwent major changes. The fiber source went from being mainly linen rags to wood, and new additives such as alum-rosin size replaced the traditional gelatin size that had prevailed since the Middle Ages. A significant decline in the durability of a large proportion of the papers made from mechanical pulp during that period was later noticed (Clapp 1972), which is nowadays common knowledge. Soon enough, great progress was made by the papermaking industry in the pulp production technologies, and it became possible to purify the pulp from wood components such as lignin. Chemical pulps from sulfite (acid) and later kraft (alkaline) cooking became available to produce better quality printing papers. Nevertheless, the papers produced during that period are among the least stable. In the twentieth century and to this day, understanding the paper degradation processes as well as studying paper lifetime has raised the interest of conservation scientists. The first attempts for modeling the cellulose degradation were led by Kuhn (1930); Ekenstam (1936); Wilson et al. (1955); Barrow and Sproull (1959). Erhardt (1989) later refined the relationship between reaction rates and temperature. From the Arrhenius equation, a 5 °C reduction in temperature doubles the lifetime of paper based on an activation energy (E_a) around 105 kJ mol^{-1}. Sebera (1994) proposed the concept of isoperm (isopermanence), a graphical representation of several relative humidity and temperature coupled values as lines that represent equal rates of deterioration and produce an equivalent effect on the permanence of paper. Later, the concept was revised by Strang and Grattan (2009) who improved the relationship between relative humidity (RH) and the equilibrium moisture content (EMC) of paper at a given temperature.

Zou et al. (1996a) developed a model for the decay of paper including acids and water concentrations as constants in the frequency factor *A* in the Arrhenius equation of the decay rate. Zervos (2010) and Porck (2000) made a substantial review of the paper degradation and its modeling. Tétreault et al. (2019) compared the decay models developed by

Ekenstam (1936), Calvini (2005), and Ding and Wang (2008), and proposed a new model based on Whatman paper no.1 paper, a cotton cellulose model paper, which included the frequency factor proposed by Zou et al. Since the pH and EMC both decreased slowly as the paper degraded, these changes were incorporated in the Zou et al. equation.

The need to model the decay of a wider range of paper types, representative of the past, present and future collections in libraries and archives, mostly printing papers with different compositions (fiber, sizing materials and mineral fillers) prompted this research. Ten papers chosen to cover this wide range were aged for different durations and at different temperatures in the presence of humidity in closed vials. Physico-chemical properties such as degree of polymerization (DP), zero-span tensile strength, pH, alkaline fillers, and equilibrium moisture content (EMC) were measured. They were used to develop a decay model based on DP, adapted to each type of paper. The aim was to achieve a better and more accurate prediction of paper decay to allow the optimization of the climate control in museums, libraries, and archives. This is particularly crucial considering the increasingly difficult challenges posed by climate change and the growing emphasis on energy efficiency of buildings housing heritage collections. These institutions are under pressure to adopt sustainable and cost-efficient practices. The output of the model developed in this research was also transposed into isoperms.

This research does not consider deacidified papers, neither the effect of inks and pigments or external pollutants on the rate of paper degradation.

Kinetic model

Some key equations used in the cellulose degradation model are summarized in this section. More detailed information on those equations can be found in Tétreault et al. (2019). The degradation of the cellulose follows first order kinetics. The most commonly used model is the one proposed by Ekenstam (1936). The non-simplified version is shown in Eq. 1. Cellulose fibers being made of orderly (crystalline) and disorderly regions, the degradation reactions occur predominantly in the latter. Sharples (1971) reported that the reaction rate is 100 times faster in the amorphous regions than in the crystalline regions. Calvini (2005) introduced the notion of levelling-off average degree of polymerization (LODP) in the Ekenstam equation (Eq. 2). LODP is an asymptotic limit in the DP decay curve, which indicates a maximum degradation of cellulose in dilute acidic conditions. Calvini et al. (2008) later proposed the concept of classes of bonds with different scission rate constants in relation to an initial number of reacting glycosidic linkages in weak, amorphous, and crystalline regions. The glycosidic bonds in each region would thus have different reactivity: weak (easily accessible and degradable), amorphous (degradation is still rather easy), and crystalline bonds (very slow). The two latter are commonly accepted to explain the experimentally verified different reactivity in the amorphous and in the crystalline regions in the literature by most authors. As for the role of weak bonds, it is most often omitted because of the claim that they may not exist as they would not resist the chemical treatments during Kraft pulp manufacturing. Only the glycosidic links in the amorphous region are relevant in this work since degradation beyond LODP will not be considered.

$$k = \frac{1}{t} ln \left[\frac{\overline{DP}_{nt}(\overline{DP}_{n0}-1)}{\overline{DP}_{n0}(\overline{DP}_{nt}-1)}\right] \quad (1)$$

$$k = \frac{1}{t} ln \left[\frac{\overline{DP}_{nt}(\overline{DP}_{n0}-LODP)}{\overline{DP}_{n0}(\overline{DP}_{nt}-LODP)}\right] \quad (2)$$

k: rate constant for glycosidic bond breakage (year^{-1})
t: time (year)
$\overline{DP}_{nt}$: Number-average degree of polymerization at time t
$\overline{DP}_{nt0}$: Number-average degree of polymerization at time zero

For simplicity, henceforth "DP" is used as an abbreviation of $\overline{DP}_{n}$.

The acid catalyzed hydrolysis reaction drives the activation energy (E_a) and frequency factor (A). Other reactions such as oxidation most likely play a secondary role and will not be considered in the present research. By using the Arrhenius empirical concept, it is possible to extrapolate accelerated ageing conditions at high temperature to long-term natural ageing at ambient temperature as shown in Eq. 4.

$$k = Ae^{-Ea/RT} \quad (3)$$

A: frequency factor (year^{-1})
E_a: activation energy (kJ mol^{-1})
R: universal gas constant (kJ mol^{-1} K^{-1})
T: temperature (K)

$$t_2 = t_1 \, e^{\left[\left(\frac{E_a}{R}\right)\left(\frac{1}{T_2}-\frac{1}{T_1}\right)\right]} \quad (4)$$

T_1: ageing temperature (K)
T_2: temperature of interest (K)
t_1: time to reach a specific change of DP at T_1 (year)
t_2: time to reach a specific change of DP at T_2 (year)

The parameter *A* in the Arrhenius equation (Eq. 3) is called the frequency factor, or the pre-exponential factor. It can be related to molecules collision and to the optimal molecular orientation for a reaction to occur. Zou et al. (1996a) decomposed the frequency factor in the cellulose degradation reaction by including in it both the concentration of hydrogen ions and the concentration of water in the paper (Eq. 5).

$$A = A_n + A_W[H_2O] + A_{WH}[H_2O][H^+] \quad (5)$$

A: overall frequency factor (year^{-1})
A_n: frequency factor for reactions not associated to hydrogen ions or water (year^{-1}).
A_W: frequency factor for reactions associated to water (year^{-1}).
A_{WH}: frequency factor for reactions associated to water and hydrogen ions (l mol^{-1} year^{-1}).
$[H_2O]$: concentration of water in paper or equilibrium moisture content (weight fraction conditioned).
$[H^+]$: concentration of hydrogen ions (mol L^{-1}).

Zou et al. (1996b) determined that A_n was about 1000 times smaller than A_W and that A_W was 10000 times smaller than A_{WH}. Because of these orders of magnitude differences, A_n and $A_W[H_2O]$ can be neglected in Eq. 5. By isolating DP_t from Eq. 2 we obtain the decrease of DP as a function of time (Eq. 6). The frequency factor (*A*) (Eq. 5) is included in the rate constant (*k*) (Eq. 3) of Eq. 6.

$$DP_t = \frac{DP_0}{\left(\frac{DP_0}{LODP}-1\right)\left(1-e^{-kt}\right)+1} \quad (6)$$

Water Concentration

The water concentration $[H_2O]$ in the paper has a direct impact on the chemical reactions. Moreover, it also has an impact on the physico-chemical processes that influence cellulose reactivity such as ion mobility, plasticity and swelling of microfibrils, which all play a role in the optimal access of the reactants to cellulose for chain scissions and are part of *A*. Sorption of water takes place mainly in the amorphous regions and the interfibrillar accessible regions. Water concentration in the paper depends on the equilibrium moisture content (EMC) of the paper, which is a function of the water vapor concentration in the surrounding environment. The Guggenheim-Anderson-de Boer (GAB) sorption equation, which represents the isotherm relation at equilibrium between the liquid and vapor phases of water was used to calculate EMC (Eq. 7) (Parker et al. 2006; Timmermann 2003).

$$EMC_{GAB} = \frac{Wm\ Km\ Cg\ RH}{(1-Km\ RH)(1-Km\ RH+Cg\ Km\ RH)} \quad (7)$$

EMC_{GAB}: equilibrium moisture content based on GAB parameters (weight fraction: g H_20/g dry sample weight)
Wm: moisture content of the monolayer (weight fraction)
Cg: Guggenheim constant related to heat of sorption
Km: constant related to multilayer molecules properties
RH: relative humidity (% x 10^{-2})

Experimental

The papers selected in this research covered a wide range in terms of fiber and non-fibrous constituents (fillers and sizing), pulping process, acidity, EMC, and DP. A code is used to identify them using letters, corresponding to the pulp type, and numbers, corresponding to the initial pH (pH_0). BKP is used for bleached kraft woodpulp, BSP for bleached sulfite woodpulp, BSGWP for the mixture of bleached sulfite and groundwood pulps, C for cotton linters pulp and TMP for thermomechanical woodpulp. To these codes, the aqueous extract pH_0 of the paper is added. Most papers were already 30 to 35 years old at the time of their use for this research and had been stored in clean (unpolluted) and T/RH controlled environment. The Whatman papers were only a few years old. The ten papers studied are described in Table 1.

Table 1 Pulp process, constituents (fibres and additives) and manufacturers of the papers studied

Paper code	Qualifier and pulp process	Fibres	Additives	Manufacturer
TMP4.7	Acid newsprint Thermomechanical pulp	Hardwood and softwood	Alum-rosin sizing	Fletcher Challenge Canada
BKP4.9	Domtar Windsor offset, acidic fine paper $^+$ Bleached kraft pulp	Hardwood and softwood	10% fillers (clay) Alum-rosin sizing	Domtar Inc.
BSGWP5.1	60% bleached sulphite pulp and 40% groundwood pulp	Softwood	20% fillers (kaolin) Alum-rosin sizing	Centre Technique du Papier
BKP5.1	Acidic fine paper Bleached kraft pulp	50% hardwood 50% softwood	4% fillers (clay) Alum-rosin sizing Starch	Domtar Inc.
C5.9	Whatman no.40, ashless quantitative filter paper	Cotton linters	none	Whatman plc (now Cytiva)
BSP6.2	Neutral fine paper Bleached sulphite pulp	Softwood	none	Swedish Pulp and Paper Research Institute
C6.5	Whatman no.1, qualitative filter paper	Cotton linters	none	Whatman plc (now Cytiva)
C8.5	AB Tumba Svenskt Arkiv 80, alkaline fine paper	80% cotton linters 20% cotton cambers	2-4% fillers (PCC) 0.5-1% TiO_2 AKD sizing	Swedish Pulp and Paper Research Institute
C9.1	Domtar Cleartone alkaline fine paper	Cotton linters	8.5% fillers (PCC) AKD sizing	Domtar Inc.
BKP9.6	Domtar Krypton Parchment, alkaline fine paper Bleached kraft pulp	15% hardwood 85% softwood	15% fillers (PCC) AKD sizing Starch	Domtar Inc.

PCC precipitated calcium carbonate; AKD alkyl ketene dimer

The paper samples were hygrothermally aged in hermetically closed vials according to TAPPI T573 pm-09 for various durations. The tensile strength, grammage, pH, EMC, and the calcium carbonate ($CaCO_3$) fillers content (alkaline papers) were measured (methods are provided in Section 1 in Supplementary Information (SI)). Based on the EMC, the GAB parameters were determined. The DP of cellulose was determined from size-exclusion chromatography analyzes of all the papers, except for those containing mechanical pulp (TMP4.7 and BSGWP5.1), for which viscosity measurements were carried out due to their poor solubility in the chromatographic solvent. The different deconvolution methods of the molar mass distribution profiles applied to obtain the number-average degree of polymerization (DP_n in Eqs 1 & 2) of the cellulose have been explained in a previous article (Dupont et al. 2018) and will not be discussed in detail here. Details on the ageing conditions and methods used for the characterizations and DP calculations can be found in Section 1 of the SI as well as in Tétreault et al. (2019).

Results

DP, zero-span tensile strength, expressed in terms of zero-span breaking length (BL), grammage, EMC, GAB parameters, pH and $CaCO_3$ content for each paper and ageing condition are reported in Table S1 in the SI. These parameters are considered one by one in the following. Note that the purpose of the present article was to determine E_a based on the experimental data and to study the relative differences between them.

Activation energy based on DP and zero-span tensile strength

Paper samples were aged at different temperatures and for various durations, their physico-chemical properties were measured, which allowed to determine their activation energy (E_a) in the Arrhenius equation. More precisely, E_a was determined based on two properties: the DP of cellulose and the zero-span breaking length (BL) of the paper. All the experimental data can be found in Table S1 (SI).

The first interesting result was that whether calculated using DP or BL, the E_a were similar within 1% to 7% (r^2 = 0.999 (Table 2). E_a(DP) will be used in the following and abbreviated E_a.

The values of E_a of all the papers tested were in the range of 93 to 130 kJ mol^{-1}. Considering the papers' pH, all the papers with an alkaline fillers (4% to 10%) had E_a around 129 kJ mol^{-1}. However, the spread of values for the acidic papers (pH ≤ 6.5) was larger, from 93 to 127 kJ mol^{-1}.

Table 2 Activation energy (E_a) (kJ mol^{-1}) based on the DP and BL

Samples	E_a(DP)	E_a(BL)
TMP4.7	101 ± 3	109 ± 1
BKP4.9	124 ± 3	129 ± 2
BSGWP5.1	104 ± 2	104 ± 2
BKP5.1	127 ± 3	125 ± 2
C5.9	93 ± 6	91 ± 10
BSP6.2	113 ± 4	120 ± 5
C6.5	102 ± 3	96 ± 11
C8.5	129 ± 2	127 ± 5
C9.1	130 ± 3	126 ± 4
BKP9.6	127 ± 4	131 ± 9

Experimental E_a from various authors, based on different paper properties (obtained with different papers and ageing conditions) are reported to be in the range 84 to 126 kJ mol^{-1} (Rouchon et al. 2016). More precisely, Zou et al. (1996a) found an E_a range of 104 – 113 kJ mol^{-1} based on the DP_v (viscometric average DP) of three acidic papers aged in

glass jars at 75% RH, maintained with NaCl solution. Liu et al. (2017) reported also a large range of E_a, from 108 to 153 kJ mol^{-1}, for ten different papers aged in various conditions in climate chambers and ovens. They reported a value as low as 37 kJ mol^{-1} for papers with iron gall ink.

In Tétreault et al. (2019), only one paper was studied: Whatman paper no.1 (same paper as C6.5). As C6.5 degraded, it was found that E_a decreased accordingly. A limit around DP 1100 was chosen as the boundary to distinguish two degradation rates. E_a of 102 kJ mol^{-1} was determined for the low degradation levels at DP higher than 1100 and E_a of 95 kJ mol^{-1} for the high degradation levels at DP lower than 1100. In the present research, the same observation was made with the two papers containing mechanical pulp, TMP4.7 and BSGWP5.1. For this reason and similarly as in Tétreault et al. (2019), it was decided to exclude the longest ageing durations from the calculation of E_a for these two papers. This progressively diminishing regime in E_a depending on the degradation state was however not found with the other papers studied.

The result of the extrapolation of the decay in DP and BL with time from high temperature ageing (Table S1 in SI) to ambient conditions (Eq. 4) are shown in Fig. 1. High initial DP or BL combined with a slow decay curve (E_a above 120 kJ mol^{-1}) yield the longest lifetimes. The time scale extends up to 1000 years on the graph but data for the three alkaline papers allow projections of DP > 500 far beyond this limit. Interestingly, while moderate DP decays are observed for the three alkaline papers, a stable zero-span tensile strength is relatively well-maintained. Papers having an E_a below 110 kJ mol^{-1} reach the LODP before 500 years (TMP4.7, C5.9 and C6.5). The half-life DP (reached at a DP loss of 50%) of C6.5 is reached in 98 years. This is in good agreement with the half-life of 103 years obtained by Jeong and Potthast (2021), which they calculated with an E_a of 88 kJ mol^{-1}. BSP6.2 shows a different decay pattern. It has a low DP_0 and an intermediate E_a of 113 kJ mol^{-1}, so its DP remains above 200 even after 1000 years with BL maintained above 7 km, for which it has the property of a durable paper.

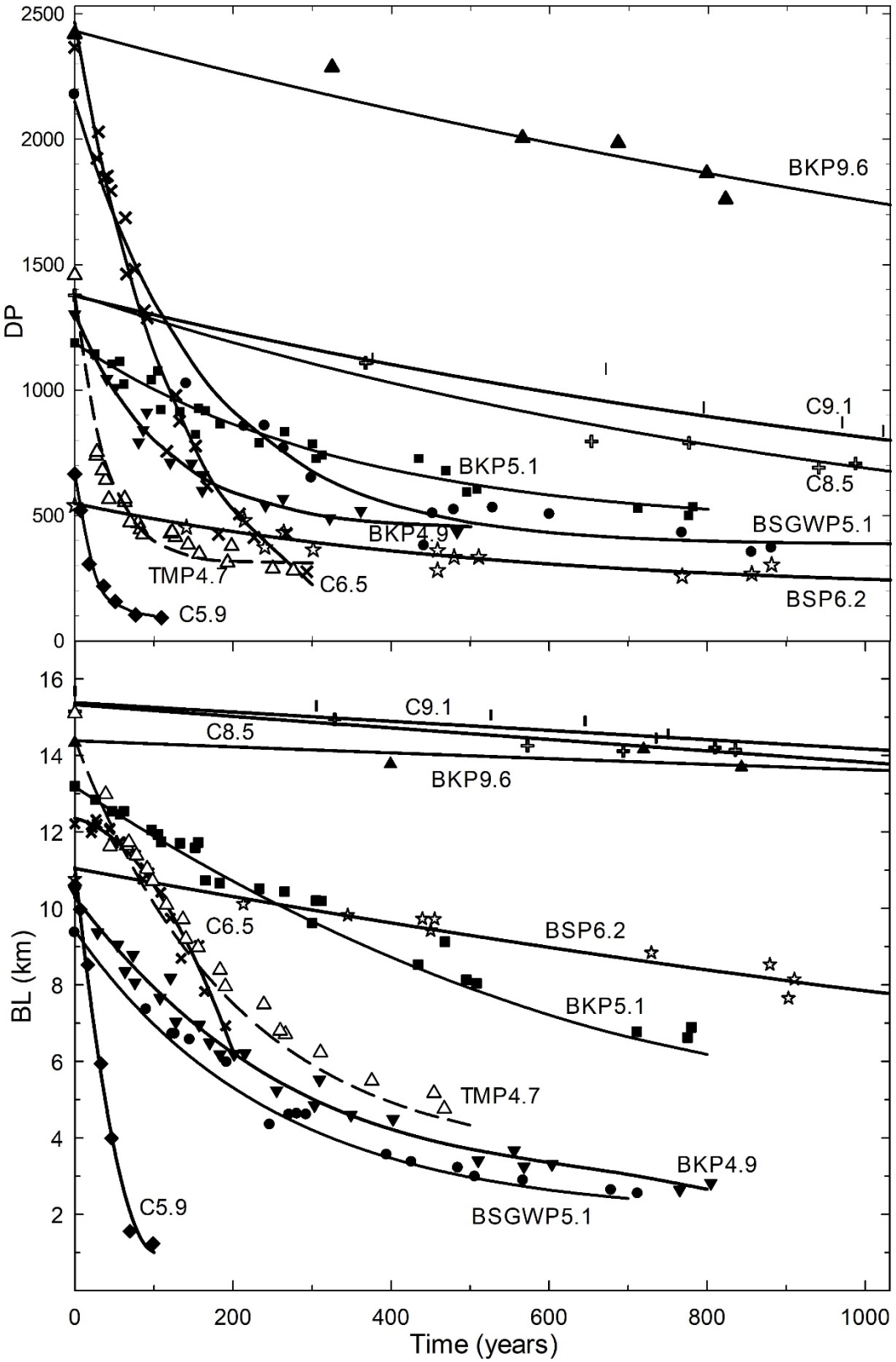

Fig. 1 DP and BL decay over time obtained by the extrapolation of artificial ageing conditions to 21 °C and 50% RH

EMC

Water concentration in the paper depends on the water vapor level in the surrounding environment. As the paper degrades, the EMC tends to decrease as shown in Fig. 2. No specific correlation was observed in terms of fiber constituents or $CaCO_3$ content. TMP4.7 and BSP6.2 stand out clearly with the highest EMC, yet it was not exactly clear why. It is also observed that for most papers, in the high DP region a substantial DP decrease is accompanied by a slow decrease in EMC. Conversely, in the low DP region 500-800, the decrease of EMC is more significant. This low DP range seems to correspond to a critical point in the degradation beyond which the decay of the paper accelerates considerably (Tétreault *et al.* 2019, Kaminska et al. 2001) as shown in Fig. S1 (SI). EMC and GAB parameters of different chemical degradation states and temperatures for all papers are in Tables S2 and S3 in the SI.

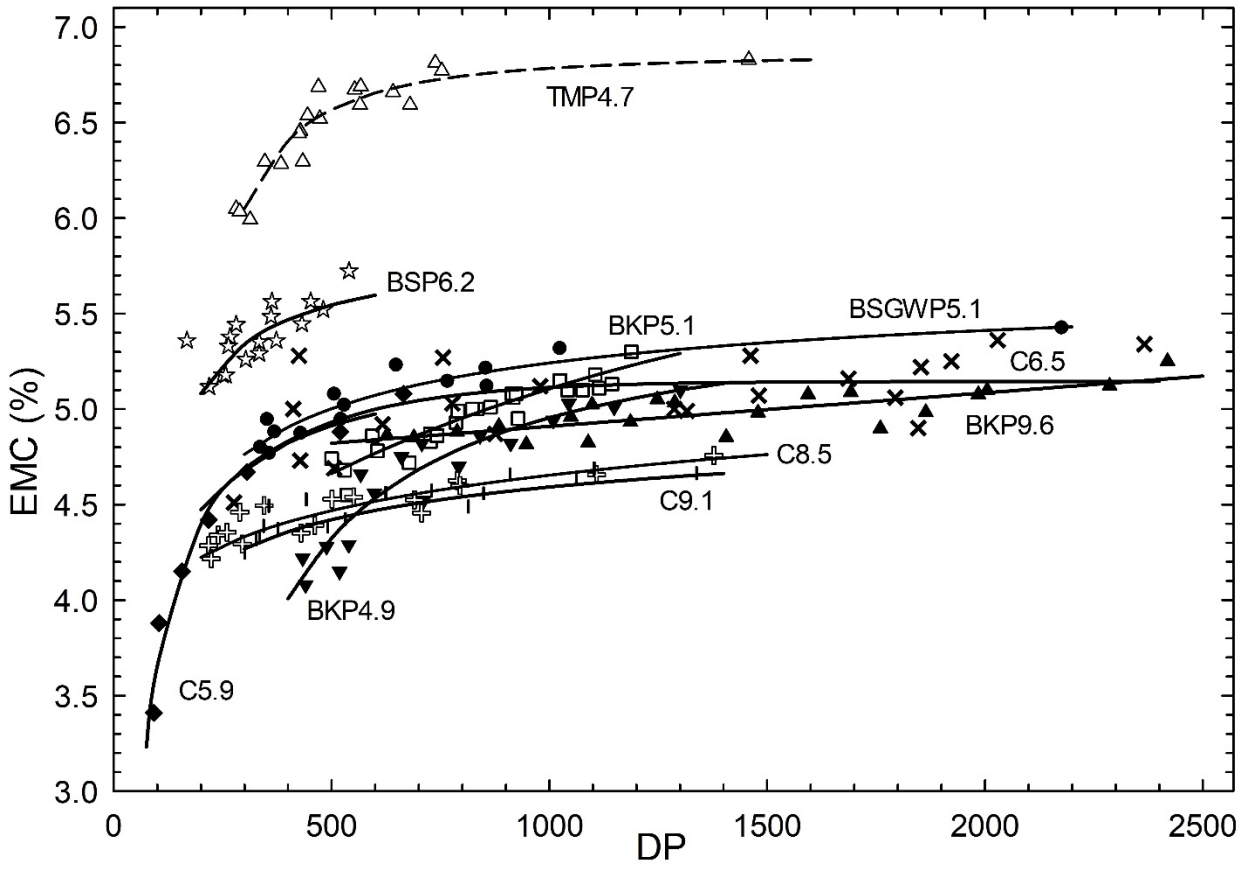

Fig. 2 Correlation between EMC (% g H_2O/g conditioned sample weight) and DP at 21 °C and 50% RH

pH

Fig. 3 shows the correlation between pH and DP, with a small decrease at high DP and a somewhat sharper one at DP below 1000. The lowest pH found, around 3.8, was for TMP4.7. It has been long known that mechanical pulp papers sized with alum-rosin acidify with time considerably more than good quality ancient papers (Barrow 1974; Jablonsky et al. 2020). The extent of the problem was underlined by Hansen and Vest (2008) who found that among a representative pool of 394 documents dating 1800-1985, 93% were acidic, the lowest pH being about 3.5, which is close to the lowest pH measured here.

Conversely, alkaline papers maintain a pH above 8 even when their DP is beyond half-life DP and has decreased from 1500-2500 to below 500. Fig. 4 shows the correlation between the pH and $CaCO_3$ content. Only unaged papers and papers aged at 100 °C for different periods of time are included. The amount of $CaCO_3$ decreased slightly (from 5% to 13%), which went along with the pH decrease as alkaline papers degraded. The dotted lines frame this trend: the top dotted line indicates the trend for all the unaged samples and the bottom dotted line the trend for all the heavily degraded papers (23 days at 100 °C). The reduction of pH in alkaline papers naturally and artificially aged was also

observed by Mochizuki et al. (2020) and Vibert et al. (2023). Bigourdan et al. (1996) suggested that the neutralization of the acids by the alkaline fillers is minor compared to their rapid generation. Bégin et al. (1998) and Hubbe et al. (2017) point out the particle size and non-uniform distribution of the alkaline fillers in the sheets being a cause of its partial inefficiency. As opposed to the results here, Vibert et al. (2022) did not detect an alkaline fillers consumption that could explain the pH decrease found in permanent paper upon ageing, and consistently with the previous authors proposed that the neutralization reaction between calcium carbonate and acids was either partial or slower than the acids production.

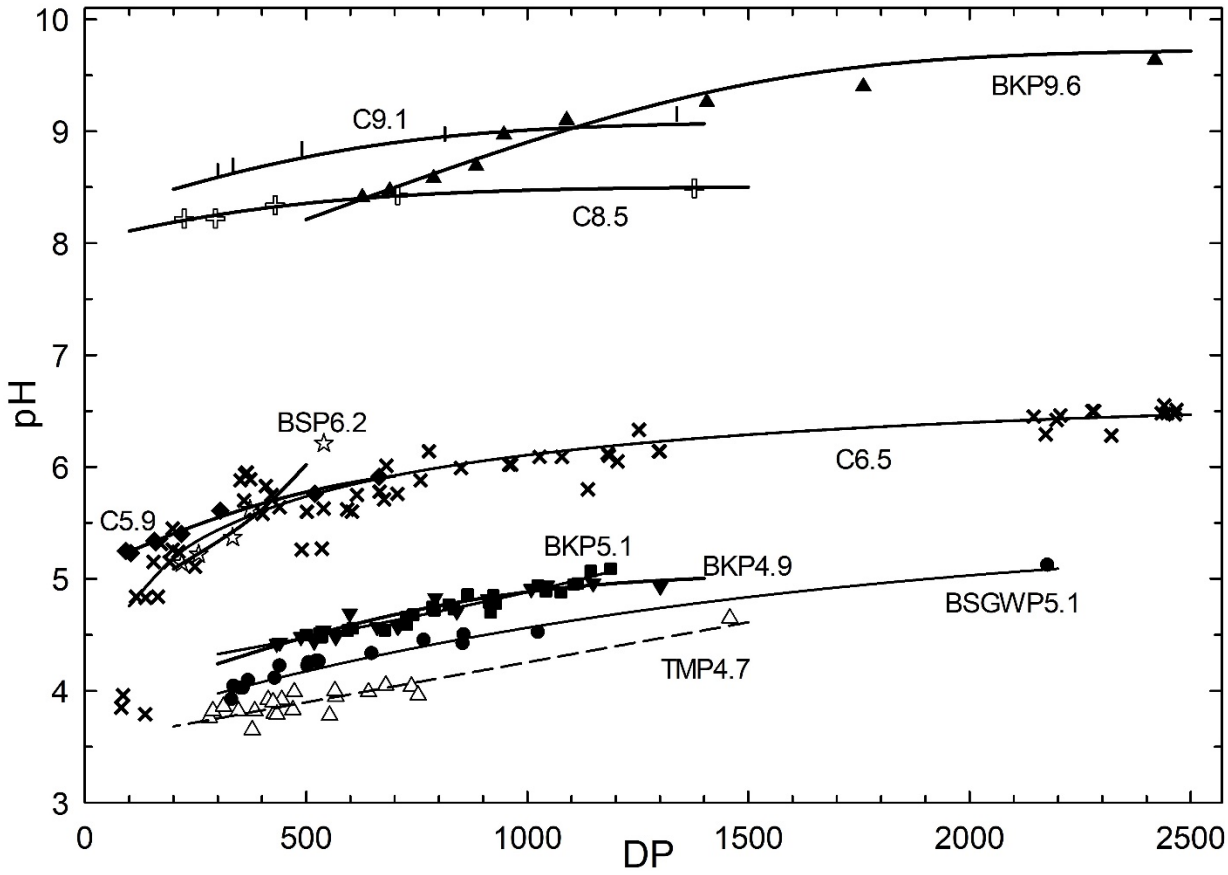

Fig. 3 Correlation between pH and DP

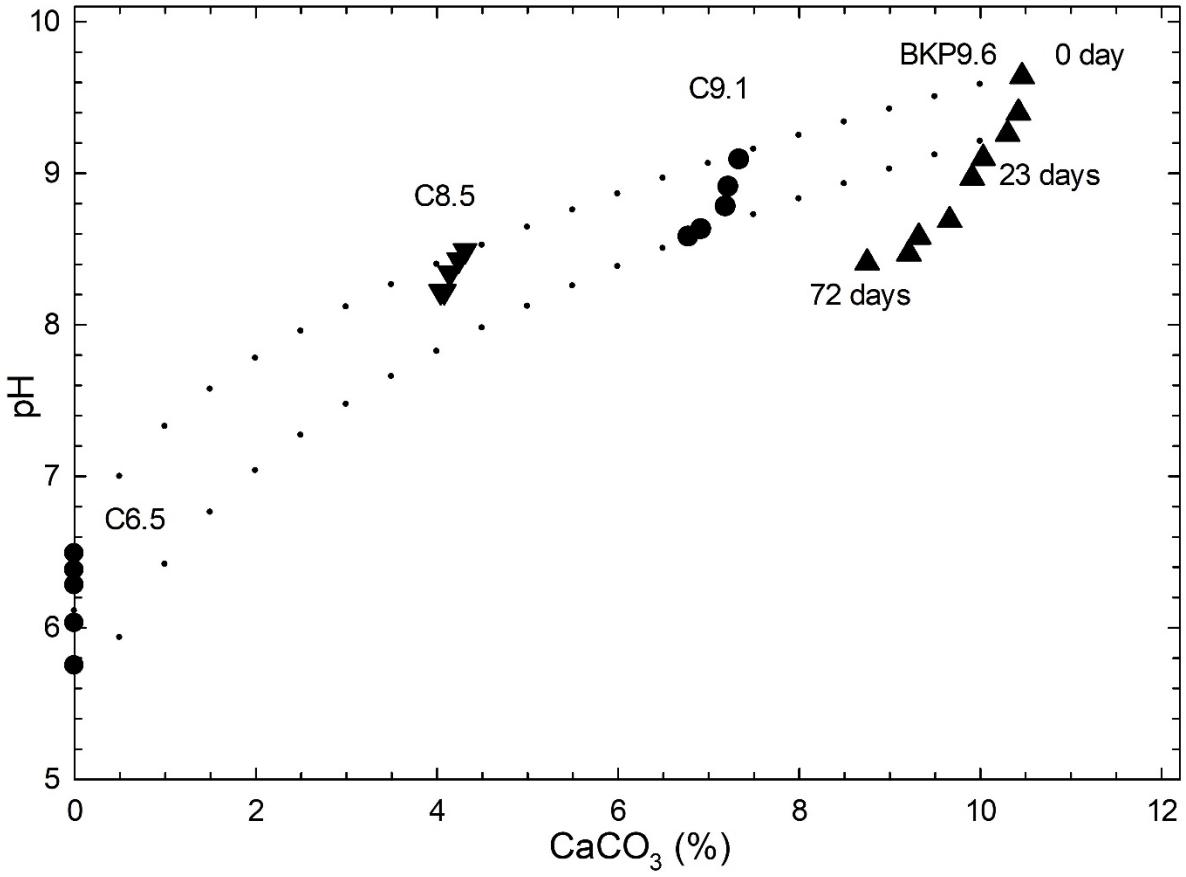

Fig. 4 Correlation between pH and $CaCO_3$ content based on paper samples aged at 100 °C for different durations up to 23 days for C8.5 and C9.1 and, 72 days (BKP9.6). The neutral C6.5 paper is presented as reference

The ISO 9706 (1994) specifies that permanent papers should contain at least 2% equivalent $CaCO_3$ as an alkaline fillers and should have a pH in the range of 7.5 to 10. Modern paper can contain up to 30% of fillers, among which kaolin and $CaCO_3$ are the most widely used (Bown 1996). A higher amount compromises fiber-fiber bonds and hence decreases the mechanical resistance. Based on Fig. 4 (dotted lines), alkaline papers should maintain a pH level at or above 7 throughout their lifetime. This supports the notion that papers containing approximately 2.5% $CaCO_3$, witch is the minimum amount of alkaline fillers in permanent paper to ensure its durability, should indeed stay in a good condition over several centuries (effects of pollutants and other agents excluded).

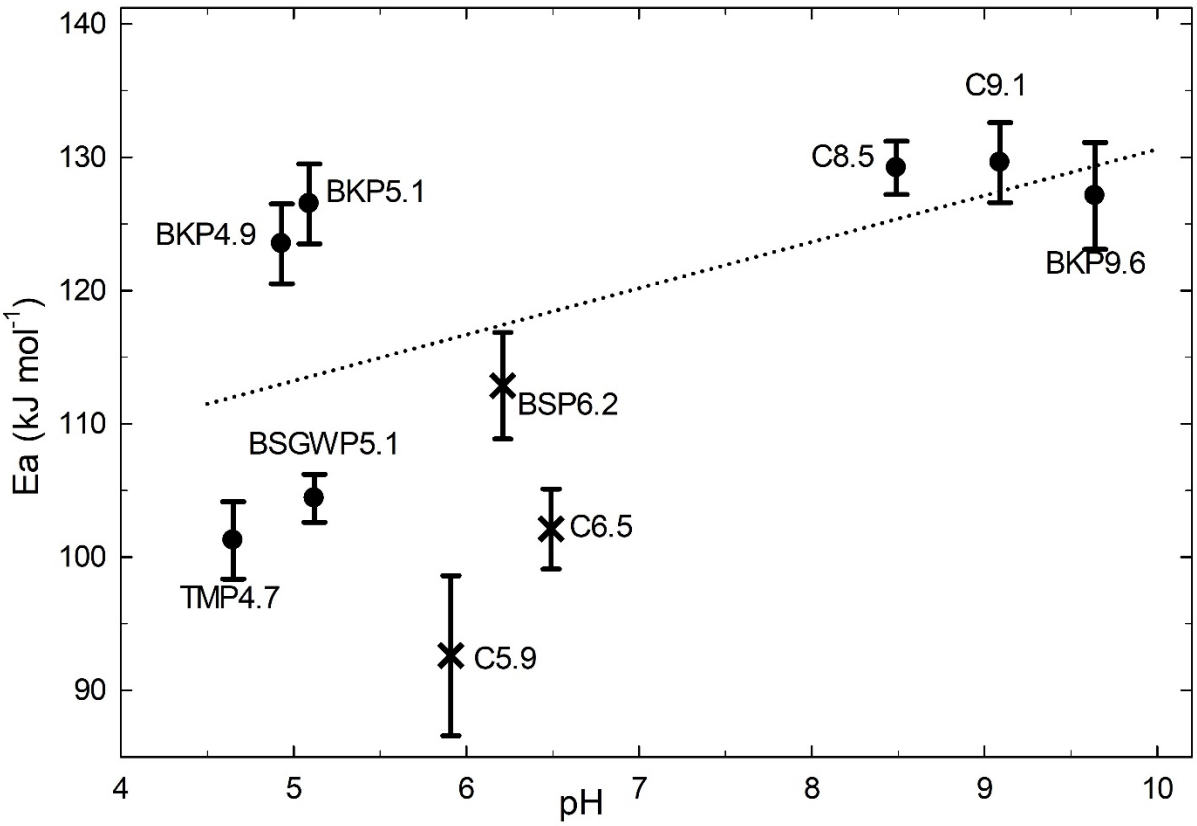

Fig. 5 E_a of all papers tested in relation with pH. X symbols are excluded from the linear relationship since they may not be considered as printing papers due to their lack of additives such as fillers and sizing

No clear relationship between E_a and pH was found among the different papers, as shown in Fig. 5. The slope shows a weak correlation even when excluding three papers on the basis that they contain no sizing nor fillers (cross symbols). However, considering only the pulping process type, it can be observed that the Ea for BKP papers is in average 126 kJ mol^{-1} independently of the pH, which tends to indicate that the alkaline fillers do not improve significantly the lifetime of BKP papers. On the other hand, the Ea of cotton linters papers increase with the pH. However, it has to be noted that C5.9 and C6.5 are model filter papers (no sizing or fillers) and they may have a different chemical reactivity than printing papers. All the papers with a high initial pH have a high E_a, as explained earlier. Above pH 7, the three printing papers made of good quality pulp (cotton linters or bleached kraft pulp) have E_a around 129 kJ mol^{-1}. On the other hand, for papers with a pH lower than 7, E_a spreads in the range 93 to 127 kJ mol^{-1}. The two kraft pulp papers (BKP4.9 and BKP5.1) have a high E_a while the papers containing mechanical pulp (BSGWP5.1 and TMP4.7) have a low E_a. BSP6.2 shows an intermediate behaviour. It is a chemical pulp (sulfite) paper, but, as pointed out before, it has an intermediate E_a of 113 kJ mol^{-1}. This could be the result of its near-neutral initial pH, and/or low initial DP. The lack of additives, especially sizing, which may also allow an easier access of water and reactants (acids) to the core of the fibers. It could also relate more broadly to the pulping process. Several theories have been proposed to account for the mechanical and chemical differences of papers produced with alkaline kraft and acid sulfite pulping processes (Young et al. 1994).

Fig. 5 also shows that for the acidic printing papers, *i.e.*, all besides C5.9, C6.5 and BSP6.2 (cross data points on Fig. 5), E_a values can be divided in two groups. For the papers that are exempt of lignin, E_a is around 126 kJ mol^{-1} and for the papers containing significant amounts of lignin (mechanical pulp), E_a is below 110 kJ mol^{-1}. This difference could be due to the lower activation energy for the hydrothermal depolymerization of lignin, which, depending on the multiple and complex reactions pathways, is reported to be in the range 32-94 kJ mol^{-1} (Zhang et al. 2008, Forchheim et al. 2014).

Isoperms

Isoperms were built for each paper, based on the time needed to reach a DP decay of 50% (half-life DP). The half-life decay was chosen instead of end of lifetime (defined as LODP) due to larger uncertainties on the predictions at high degradation states.

For example, according to our decay model, it would take 630 years for paper BKP5.1 to reach half-life DP at 50% RH and 20 °C. The duration of 630 years defines the isoperm 1 for this paper as shown in Fig. 6. When the isoperm moves from line 1 to 2, the decay rate decreases by a factor of 2 meaning that it will take twice as long to reach the DP decay of 50%. All the papers studied follow similar isoperm plots. This notion is developed in another section below. Isoperm curves in Fig. 6 are similar as reported by Strlič et al. (2015). Isoperm lines in Sebera's (1994) are more vertical towards high RH. Despite this, and consistently with the isoperm of Strlič et al. (for papers having a pH = 8) and Sebera (for papers with an enthalpy of activation of 105 kJ mol^{-1}), our data show the same shift from isoperm 1 to 25 when environmental conditions change from 50% RH and 20 °C to 20% RH and 5 °C.

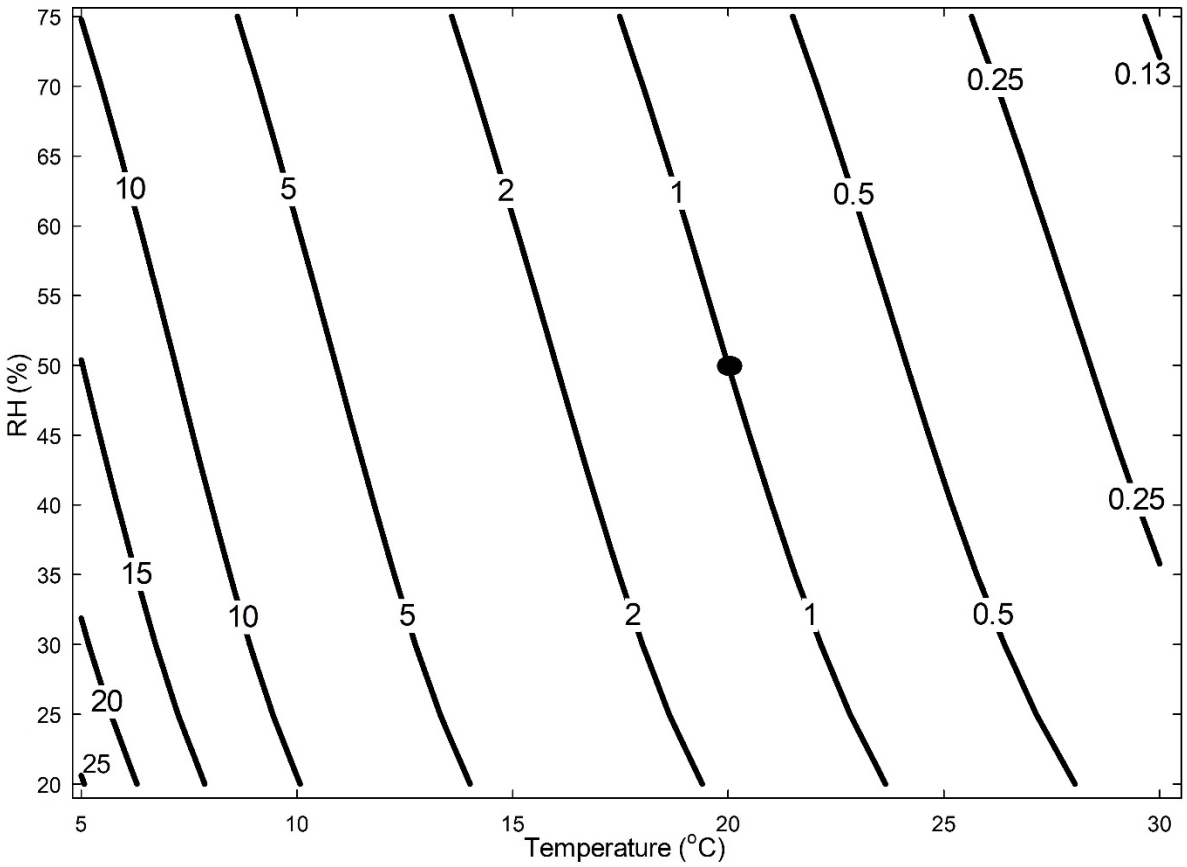

Fig. 6 Isoperm diagram of the paper BKP5.1

Model development and simulation

Empirical equations for the kinetic model

Further correlations between the chemical parameters were needed for completing the model developed by Tétreault et al. (2019). Different empirical mathematical correlations must be determined for each paper such as EMC, pH and A_{WH} as a function of DP.

EMC

The GAB equation (Eq. 7) allows to determine the relationship between EMC and RH for a given paper at a specific temperature. The GAB parameters obtained at 10, 21 and 30 °C (Table S2 in SI) as a function of the temperature followed a second-degree polynomial fit defined with a curve fit program (TableCurve 2D v5.01). The parameters in Eq 7 could then be defined. Those results are shown in Table 3. GAB parameters as a function of temperature for C6.5 and C5.9 had been already determined in Tétreault et al. (2019). Equations in Table 3 should remain valid slightly beyond the temperature range used due the smooth trends of the fitted curves.

Table 3 GAB parameters as a function of the temperature T in Kelvin and the parameter moisture adjustment (*Ma*) used in the correlation between EMC and DP

Samples	*Cg*	*Km*	*Wm*	*Ma*
TMP4.7	$-2.015 \times 10^{-3}T^2 + 0.9620T - 99.90$	$-2.280 \times 10^{-4}T^2 + 0.1327T - 18.53$	$1.709 \times 10^{-5}T^2 - 0.01028T + 1.602$	4.500×10^{-3}
BKP4.9	$1.762 \times 10^{-3}T^2 - 1.245T + 223.5$	$-2.970 \times 10^{-5}T^2 + 1.647 \times 10^{-2}T - 1.476$	$-1.237 \times 10^{-6}T^2 + 5.980 \times 10^{-4}T - 3.027 \times 10^{-2}$	4.500×10^{-3}
BSGWP5.1	$3.540 \times 10^{-4}T^2 - 0.4460T + 109.7$	$-2.352 \times 10^{-4}T^2 + 0.1362T - 18.94$	$1.279 \times 10^{-5}T^2 - 7.619 \times 10^{-3}T + 1.178$	2.050×10^{-3}
BKP5.1	$3.620 \times 10^{-3}T^2 - 2.366T + 392.4$	$-6.636 \times 10^{-5}T^2 + 3.804 \times 10^{-2}T - 4.663$	$1.753 \times 10^{-6}T^2 - 1.139 \times 10^{-3}T + 0.2234$	5.000×10^{-3}
BSP6.2	$5.303 \times 10^{-5}T^2 - 0.2203T + 69.33$	$-7.525 \times 10^{-5}T^2 + 4.337 \times 10^{-2}T - 5.466$	$2.510 \times 10^{-6}T^2 - 1.638 \times 10^{-3}T + 0.3102$	4.400×10^{-3}
C6.5 & C5.9	$0.7161\ e^{(7.389 - 0.01749T)}$	$1.034\ (0.8169 - 2.852 \times 10^{-9}T^3)$	$0.8227\ (0.1135 - 2.160 \times 10^{-4}T)$	0.795×10^{-3}
C8.5	$4.693 \times 10^{-3}T^2 - 2.959T + 473.4$	$-5.970 \times 10^{-5}T^2 + 3.449 \times 10^{-2}T - 4.175$	$1.515 \times 10^{-8}T^2 - 1.624 \times 10^{-4}T + 8.378 \times 10^{-2}$	1.500×10^{-3}
C9.1	$-4.333 \times 10^{-4}T^2 + 1.633 \times 10^{-4}T + 47.51$	$-6.869 \times 10^{-5}T^2 + 3.957 \times 10^{-2}T - 4.876$	$1.182 \times 10^{-6}T^2 - 8.059 \times 10^{-4}T + 0.1696$	2.200×10^{-3}
BKP9.6	$2.444 \times 10^{-3}T^2 - 1.665T + 288.8$	$-5.838 \times 10^{-5}T^2 + 3.355 \times 10^{-2}T - 4.013$	$2.303 \times 10^{-6}T^2 - 1.512 \times 10^{-3}T + 0.2859$	3.000×10^{-3}

It was found that EMC decreases as the DP decreases, as shown in Fig. 2. The empirical equation developed for C6.5 and validated in Tétreault et al. (2019) modelled the change in EMC as paper degrades. The Eq. 9 developed by Tétreault et al. (2019) integrates this evolution based on the number of broken glycosidic bonds (n) (Eq. 8). In Eq. 9 the moisture adjustment parameter (*Ma*) is unique to each paper, and determined with the curve fit program. It replaces the value determined for C6.5 in Tétreault et al (2019). *Ma* for each paper is reported in Table 3. Fig. 7 represents the result of a simulation for the paper BKP5.1. It shows the importance of continuously adjusting the EMC input in the model. As the DP decreases (paper degrades or is exposed to high temperature), the isotherm is shifted downwards, which in turns affects the degradation rate. The two experimental data points shown in Fig. 7 (grey diamond symbols) fall exactly on the simulated curve and validate the Eq. 9

$$n = \frac{DP_0}{DP_t} - 1 \quad (8)$$

n: number of broken glycosidic bonds
DP_0: DP at time zero (unaged)
DP_t: DP at time t

$$EMC_{DP} = EMC_{GAB}\ \frac{EMC_0 - Ma\left(\frac{DP_0}{DP_t} - 1\right)}{EMC_0} \quad (9)$$

EMC_{DP}: EMC as a function of DP_t (%) (weight fraction: g H_20/g dry sample weight)
EMC_{GAB}: EMC based on GAB equation (as a function of temperature) (weight fraction)
EMC_0: EMC of unaged paper at 21 °C and 50% RH (weight fraction)
Ma: Moisture adjustment factor (weight fraction)

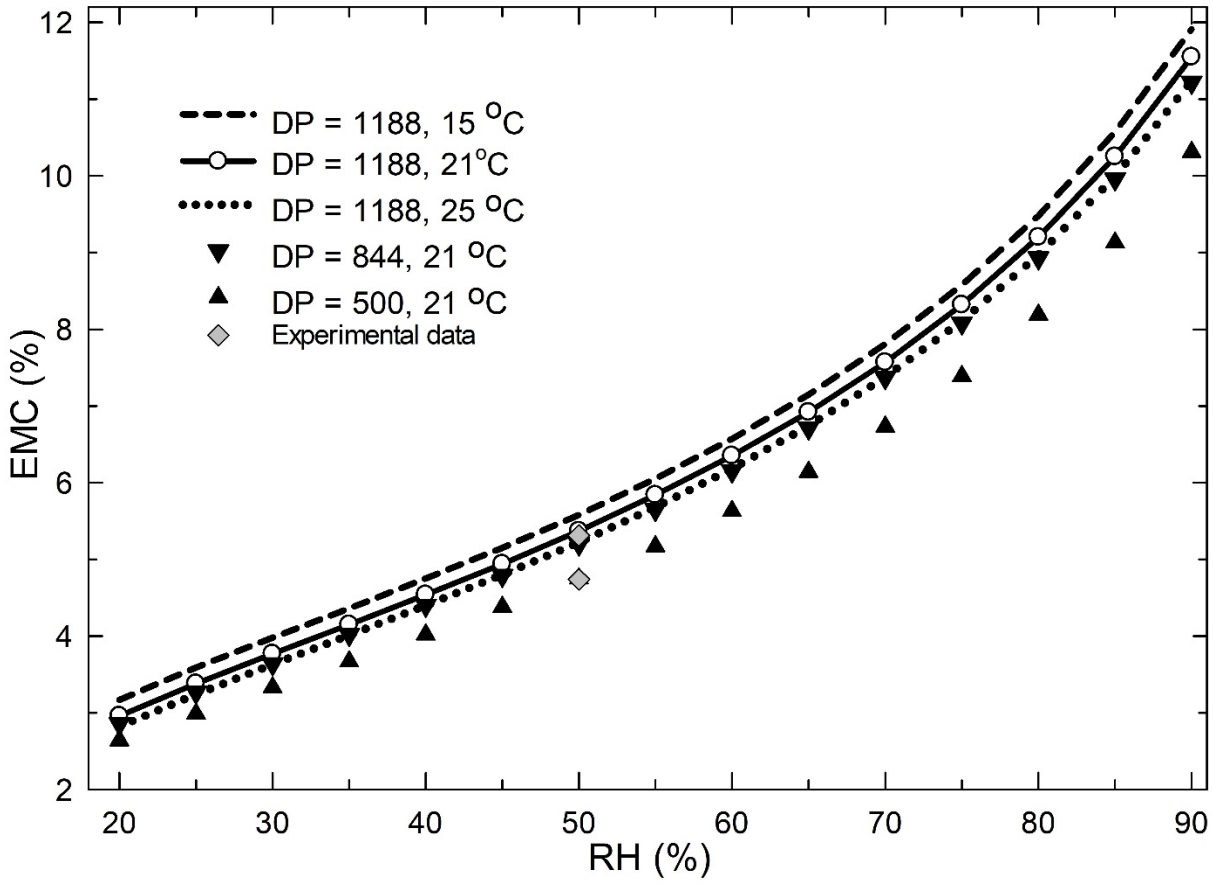

Fig. 7 Simulated EMC of BKP5.1 (% g H_2O/g conditioned sample weight) as function of RH for different temperatures and DP. Grey diamond symbols are experimental data for DP = 1188 and 500 at 21 °C and 50% RH

pH

From the relationship between pH and DP (Fig. 3) a generic equation (Eq. 10) was determined that relates the concentration in hydrogen ions $[H^+]$ to DP_t. The parameters a, b, and c of the equation were determined with the curve fit program and are provided in Table 4. This equation fitted well all the papers, but less so the most degraded C6.5 (DP<400). Eq. 11, which had been developed in Tétreault et al. (2019), gives a better fit for C6.5, especially for DP below 400. The Eqs. 10 and 11 shown as trendlines in Fig. 3 fit well the experimental data.

$$[H^+] = a + be^{\left(-\frac{DP_t}{c}\right)} \quad (10)$$

$$[H^+] = \frac{0.000730}{(DP_t - 100)} \quad (11)$$

Table 4 Parameters in the relationship pH as a function of DP (Eq. 10) for each paper

Samples	a	b	c
TMP4.7	-4.156×10^{-5}	2.705×10^{-4}	1009.4
BKP4.9	8.848×10^{-6}	1.378×10^{-4}	287.1
BSGWP5.1	7.231×10^{-6}	2.388×10^{-4}	352.1
BKP5.1	-5.249×10^{-6}	8.177×10^{-5}	669.6
C5.9	8.836×10^{-7}	7.582×10^{-6}	221.3
BSP6.2	-1.482×10^{-6}	2.356×10^{-5}	222.9
C6.5	3.800×10^{-6}	9.200×10^{-6}	316
C6.5[a]	1.828×10^{-7}	1.439×10^{-2}	-1.460
C8.5	3.106×10^{-9}	6.428×10^{-9}	313.7
C9.1	8.190×10^{-10}	4.946×10^{-9}	290.4
BKP9.6	1.864×10^{-10}	3.326×10^{-8}	290.9

[a] Eq.11 is used for C6.5

A_{WH}

In Tétreault et al. (2019) it was observed that the predicted decay of C6.5 was faster than the degradation measured experimentally. The most likely explanation is that the concentration of hydrogen ions predicted by the model at low DP was too high. It was proposed that the contribution of the hydrogen ions in the depolymerization is less efficient as the paper becomes more degraded. An adjustment was applied for simplicity by decomposing A_{WH} as shown in Eq. 12. This observation was confirmed with all the papers tested in this research, which indicates that this is a common phenomenon in the degradation of paper. Using the same approach as for C6.5, A_{WH_1} and A_{WH_2} were determined with a best fit method (Excel program) and are shown in Table 5. This adjustment allowed to fit the output that as DP decreases, A_{WH} is slowly reduced. This equation can be used until it becomes clearer what is or are the factors affecting the decrease in the degradation rate with the ageing of paper and can be refined further.

$$A_{WH} = A_{WH_1} - A_{WH_2}\, e^{\left(\frac{DP_0 - DP_t}{DP_0}\right)} \quad (12)$$

A_{WH_1} and A_{WH_2}: partial frequency factors for reactions associated to water and hydrogen ions.

Table 5 Partial frequency factors (l mol^{-1} year^{-1}) used for the Eq. 12

Samples	A_{WH_1}	A_{WH_2}
TMP4.7	1.30×10^{21}	5.30×10^{20}
BKP4.9	1.70×10^{25}	7.80×10^{24}
BSGWP5.1	5.20×10^{21}	2.07×10^{21}
BKP5.1	1.60×10^{25}	7.50×10^{24}
C5.9	1.13×10^{22}	4.80×10^{21}
BSP6.2	5.60×10^{23}	2.60×10^{23}
C6.5	3.20×10^{22}	7.70×10^{21}
C8.5	6.20×10^{28}	1.20×10^{28}
C9.1	1.60×10^{29}	3.80×10^{28}
BKP9.6	1.10×10^{29}	5.50×10^{28}

BL vs DP

Both DP and BL show an exponential decay over time, but a linear correlation between BL and the number of broken glycosidic bonds (*n*) (Eq. 8) is found, as shown in Fig. 8. The conversion of DP to BL is then made easier through the number of broken glycosidic bonds as shown in Eq. 13. Parameters d (slope in km) and BL_0 are in Table S4 in SI. A deviation from the linear correlation was observed only for C5.9 because of the level-off degree of polymerization (LODP) being reached, as shown by the grey diamond symbols.

$$BL = -d\,n + BL_0 \quad (13)$$

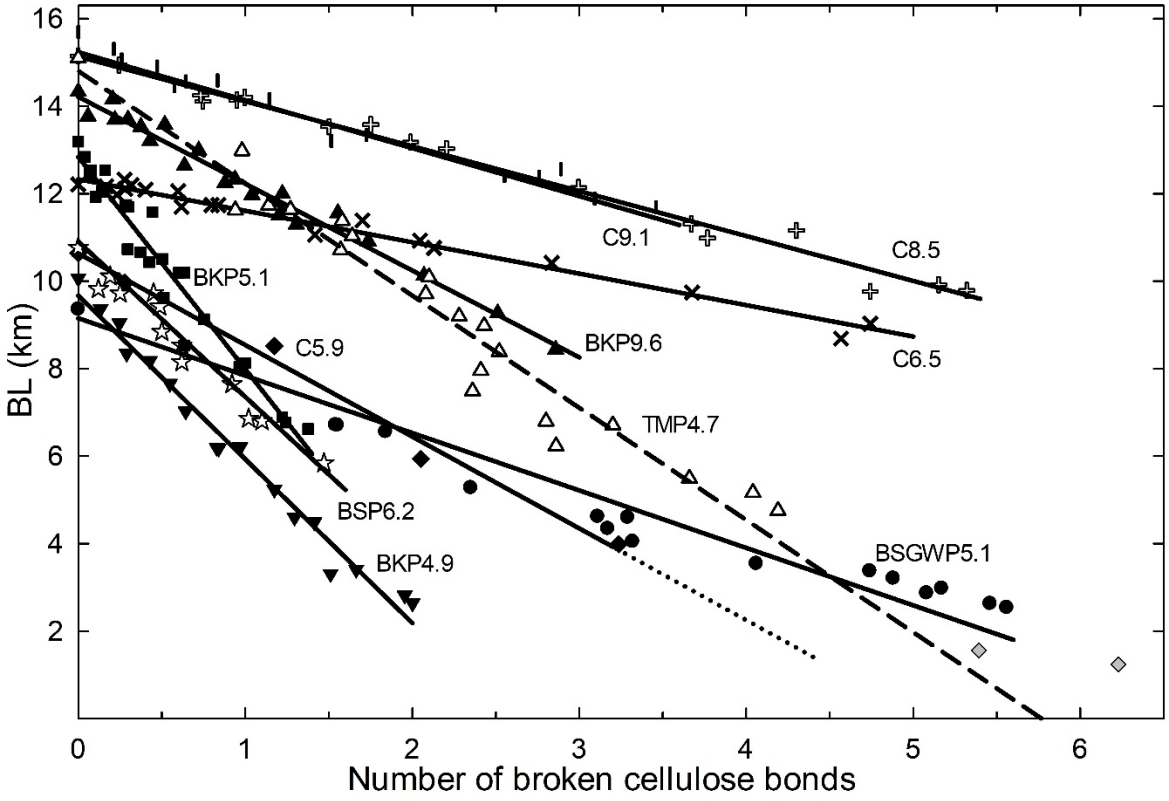

Fig. 8 Correlation between BL and number of broken cellulose bonds (*n*)

Isoperms

A generic isoperm model based on the papers studied in this project was developed. Both the RH and temperature are included in the isoperm equation (Eq. 14). The exponential segment on the right refers to the change of temperature based on the Arrhenius equation (Eq. 4) and the exponential segment on the left, including the factor 2.46, refers to the change of RH. The change of RH is modelled with a best fit equation developed based on BKP4.9 data. BKP4.9 was chosen since its relationship EMC vs RH is average, hence a conservative representation of the different papers studied as shown in Fig. 2. At 50% RH and 20 °C, the isoperm (Eq. 14) of 1.0 is obtained. This is the reference point. As the RH and/or temperature change, the isoperm will reflect the new decay rate independently of the type of paper. The isoperm model closely fits the experimental data of the different papers tested with their respective E_a but independently of their pH. However, the difference between the experimental data and the modelled data increased up to 15% if extreme environmental conditions were applied such as cold and dry or warm and humid.

$$\text{Isoperm} = 2.46\, e^{(-(0.00822T_2 - 0.572)RH)}\, e^{\left[\left(\frac{E_a}{R}\right)\left(\frac{1}{T_2}-\frac{1}{T_1}\right)\right]} \quad (14)$$

RH: relative humidity of interest (fraction)

T_1: temperature of reference: 293.15 Kelvin
T_2: temperature of interest (Kelvin)

Hygrothermal degradation simulation

DP Decay simulation

The integration of DP, EMC and pH determined experimentally into each paper's respective equation allows to simulate their decay. This is shown in Fig. 1 where the decay curves drawn to fit the experimental data points are the result of the model simulation. Fig. 9 shows the results of decay simulations for TMP4.7, BKP5.1, BKP9.5 and C6.5 in different climate conditions. These simulations are based on non-fluctuating temperature and RH. Indeed, the cycling of these parameters during accelerated ageing have been shown to have little impact. The fluctuation between 55 and 75% RH or 84.2 and 95 °C have been shown to have no significant impact on the long-term decay of different papers (Menart et al. 2011). Shahani et al. (1995) and Bogaard and Whitmore (2002) had found an impact of RH fluctuations, yet over a larger RH span (40 % to 90% RH at 40 °C and 25% to 75% RH at 23 °C, respectively). The simulations also do not consider any additional adverse effect due to external or indoor air pollutants, which have been shown to degrade paper (Tétreault et al. 2013).

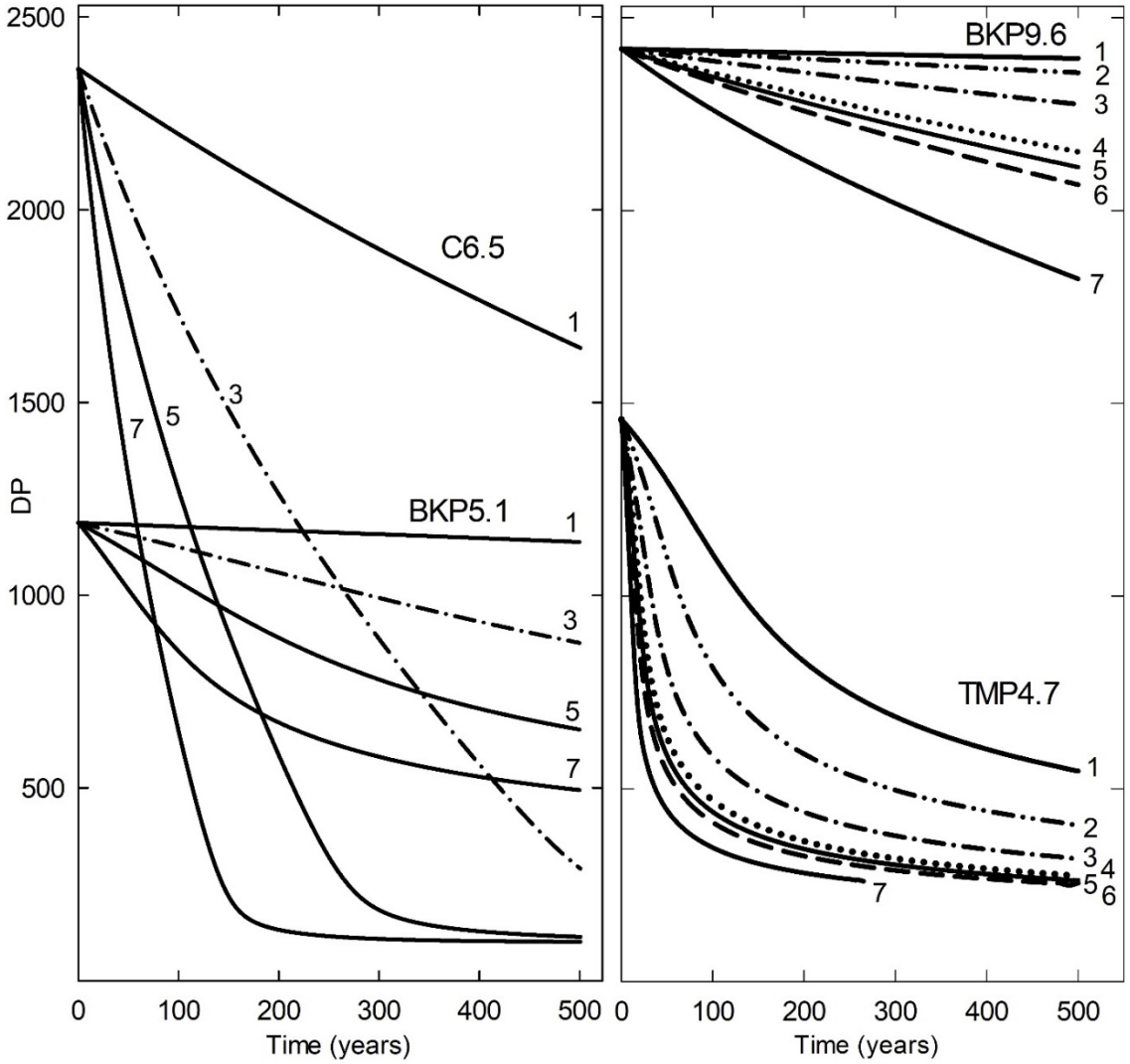

Fig. 9 Decay simulations for TMP4.7, BKP5.1, C6.5 and BKP9.6 in different environmental conditions. Line 1: 50% RH & 5 °C; 2: 50% RH & 10 °C; 3: 50% RH & 15 °C; 4: 40% RH & 20 °C; 5: 50% RH & 20 °C; 6: 60% RH & 20 °C; 7: 50% RH & 25 °C

The decay trends at the different ambient conditions support the recommendation for archives to store paper documents in dry and cold environment for best preservation. The contributions of the temperature and RH in the cellulose degradation are shown in the Arrhenius equation (Eq. 3) and the equation defining the frequency factor *A* (Eq.5). Since the temperature is an exponent in the Arrhenius equation, at constant E_a, a small reduction in temperature will result in a bigger reduction of the paper decay than the same small reduction of the RH. This is illustrated in Fig. 9 for TMP4.7 and BKP9.6.

Fig. 9 further demonstrates that papers with an E_a of 120 kJ mol^{-1} or higher, such as those containing at least 2% $CaCO_3$ alkaline fillers (BKP9.6) or other kraft quality papers (BKP5.1), would experience a very different loss of DP, of about 10% and 50%, respectively, when stored under conditions of 60% relative humidity (RH) and 20-22 °C for a period of 500 years. At the opposite end, papers with E_a lower than 110 kJ mol^{-1} such as TMP4.7 and C6.5 or with an initial DP lower than 1000 will need stricter environmental control to maintain their DP above the LODP over 500 years. For example, with E_a of 101 kJ mol^{-1}, TMP4.7 should be stored at or below 10 °C and 50% RH or 15 °C and 20% RH.

It is interesting to compare the simulated decay of BKP5.1 and TMP4.7. They have a similar pH_0 but different E_a (127 and 101 kJ mol^{-1}, respectively). In this case, after 250 years, the loss of DP for BKP5.1 and TMP4.7 is 48 and 82%, respectively, showing that in this case E_a drives the durability property. The compared simulation decay of BKP5.1 and BKP9.6 indicating a different pattern. They have a have similar E_a (127 kJ mol^{-1}) but different initial pH_0. The simulation revealed that the DP of BKP5.1 drops by 58% after 500 years in the least favorable environment conditions (conditions 7: 50% RH and 25 °C) while DP of BKP9.6 dropped by only 28% as shown on Fig. 9. This points out that pH also plays a role in the durability for those papers. This is explained by the respective contributions of E_a and pH_0 to the decay model. As shown in Eqs. 3 and 5, E_a and pH_0 are expressed as natural and decimal logarithms, respectively. A small change in their values causes a great impact. For example, for TMP4.7, a 3% increase of the E_a and pH_0 yields a DP difference of 71% and 28%, respectively. The impact of E_a errors on the decay simulation of TMP4.7 can be viewed in the Fig. S2 in the SI.

TMP4.7 and C6.5 also have a similar E_a (101 and 102 kJ mol^{-1}) and different pH_0. However, after 250 years, they show a rather similar loss of DP of 82% and 95%, respectively. Both approach their respective LODP, yet C6.5 has a higher initial DP_0 of 2366, while DP_0 of TMP4.7 is 1458, i.e., 50% lower. With DP_0 and pH_0 higher than TMP4.7, a better durability of C6.5 was expected. This lack of performance may be due to the absence of papermaking additives (dry strength agents, sizing) compared to a printing paper. Of course, a paper with low E_a and low pH_0 will decay much faster than any paper with higher E_a and/or pH_0. This is the case for instance with TMP4.7 and BSGWP5.1 as illustrated in Fig. 1.

Based on the simulation and excluding the two Whatman model papers, the following observations can be made: both E_a and pH_0 are critical parameters that determine the durability of paper but weigh differently depending on the paper. Already in 1978, Gray (1978) supported that pH alone could not allow to estimate paper lifetime with confidence. A decay model based on a unique E_a and different pH_0 may be valid, but only for the same type of papers (Strlič et al. 2015), and not for different types of papers with varied characteristics.

Of course, different parameters such as EMC, metal ions salts such as alum (Barański et al. 2004) and grammage (high grammage tends to be associated with higher tensile strength) also affect the paper decay rate to some extent. It is worth noting that although their individual contributions may contribute to the decay, their collective impact are most likely integrated into the overall E_a value as determined here.

The model proposed is built using new papers, but it also allows the simulation of the decay over time of papers which are already naturally aged and somewhere along their DP decay. For instance, if TMP4.7, which has a DP_0 of 1458 was aged naturally at 50% RH and 20 °C for 100 years, its DP would be expected to be 440, as illustrated in Fig. 9. Using the age information, the simulation can start at a DP of 440, and the corresponding adjustments will be made automatically with the relationships between DP, EMC, pH, and A_{WH} developed above. This ensures that the simulation always accurately reflects the changes that occur in the paper as it ages.

Using Eq. 13 a simulated DP can allow to determine a respective BL for each paper, as shown in Fig. 8. When DP is below about 300, BL becomes as low as 2.5 km, which also sets the limit of the linearity of the relationship between

BL and the number of broken glycosidic bonds. For C6.5 a good linearity is maintained until the DP reaches 150, which is close to its LODP of 100 (Tétreault et al. 2019). A physical strength threshold can be associated to DP close to LODP. A BL higher than 3 km could thus be considered best for safe handling of different type of papers.

Scenario based on isoperms

Two scenarios based on the impact of the reduction of temperature and RH were investigated using the isoperm generic model (Eq. 14). Table 6 shows the impact of the decrease of 5 °C on the isoperm based on different E_a. A decrease of 5 °C doubles the lifetime of papers with E_a of 95 kJ mol^{-1}. The higher the E_a, the better is the permanence. This means for instance that papers containing mechanical pulp would need to be stored at lower temperature than chemical pulp papers in order to significantly increase their lifetime. Table 7 shows the impact of reducing the RH by half on the isoperm. The isoperm almost doubles (× 1.9) when the RH is reduced from 70% to 35%, and this was verified for any given E_a. Table 7 also shows that by halving RH in the lower RH range, the improvement in the isoperm is smaller. Moreover, the isoperm increase with the RH reduction was practically the same at any temperature. The data in Strlič et al. (2015) and Parsa Sadr et al. (2022) indicated a higher increase, by a factor of about 3.4 in the same conditions, i.e., when halving RH from 70% to 35%, independently of the pH of their paper. Even though the values are in the same order of magnitude, it is important to keep in mind that the approach of these authors differs from ours in several ways, including a different isoperm 1 setting and model used. It is worth noting that while the E_a and pH_0 values are crucial, the uncertainty on these values have a negligible impact on the two scenarios cited above, as this is a relative comparison. The Isoperm equation (Eq. 14) is a useful tool that can be applied to different papers, even in cases where the E_a is unknown. The impact of E_a on the isoperm is relatively small, which means that the average E_a for each type of paper can be used. For example, in the case of mechanical pulp papers, bleached kraft pulp papers, and papers with alkaline fillers, average values of 103, 125, and 129 kJ mol^{-1}, can be used respectively.

Table 6 Effect of E_a and temperature on isoperm at 50% RH

E_a (kJ mol^{-1})	Temperature (°C)	Isoperm
95	20	1.0
95	15	2.0
110	20	1.0
110	15	2.2
130	20	1.0
130	15	2.6

Table 7 Effect of RH on isoperm at 20 °C

RH reduction	Isoperm increase	Permanence increase
70% to 35%	0.7 to 1.3	1.9
60% to 30%	0.8 to 1.4	1.7
50% to 25%	1.0 to 1.6	1.6

In Du Plooy (1981) the permanence of acid and alkaline papers was found to improve by a factor of 17 when the environmental conditions shifted from 50% RH and 20 °C to 30% RH and 10 °C. This projection is twice as optimistic. With the isoperm developed here, an improvement of about 8 times was obtained, and a similar result was obtained by Strlič et al. (2015). Du Plooy also claimed an improvement of the permanence of about 1000 and 500 for acid and alkaline papers, respectively, if the conditions shifted further down to 5% RH and 5 °C. Again, our isoperm shows a more modest improvement of 70 and 60, respectively. A slight extrapolation of the isoperm developed by Strlič et al. (2015) tends to a similar result.

As with any prediction, the decay model developed is not without limitations and uncertainties. One such limitation is the relatively small number of papers studied (10), which restricts the projections made based on some of the observations. However, our results are consistent with previously published results which strengthens the confidence on their reliability. The relative change in decay rates resulting from variations in the environment conditions is likely to be more reliable than determining a DP value reached after an extended period of time.

Conclusion

The application of the decay model developed in Tétreault et al. (2019) to different types of paper allowed to confirm its validity beyond the proof of concept for a wide range of papers as well as making the following new observations.

The integration of DP, EMC, and pH into the Calvini kinetic model enables the prediction of the decay rate of different types of papers under different environmental conditions for an extensive period of time, i.e., over several centuries. If all the simulations in this research rely on new or quasi new paper, they also apply to naturally aged printing papers as long as their actual DP_t at the time of the simulation is taken into consideration. The time to reach their end lifetime is obviously shorter
.

A wide range of E_a was found for the papers, from 93 to 130 kJ mol^{-1}. Papers with alkaline fillers have an E_a around 129 kJ mol^{-1}. All the bleached kraft pulp papers also have an E_a around 126 kJ mol^{-1} even those with low (acidic) pH_0. Their high E_a ensures their durability. However, the mechanical pulp papers have an E_a below 110 kJ mol^{-1}, which, as demonstrated threatens their lifetime. Two Whatman papers made of cotton linters, used as models, showed a low E_a of 93 and 102 kJ mol^{-1} compared to the other papers. These two papers widely used as paper models in several paper ageing studies therefore show their limitations in terms of representativeness of printing papers and archival papers for durability studies.

Secondary to E_a, the simulations show that pH_0 is also a critical parameter that determines paper decay and hence its durability. However, the accurate determination of the end of lifetime remains a challenge for any decay model due to the uncertainty on E_a, which is inherent to the experimental parameters, as well as because of the hardly predictable future environmental conservation conditions.

The model allowed the development of a generic isoperm, based on E_a, valid for a wide range of papers made of different fibers and additives, and different pH_0, which represent the modern paper collections presently stored in libraries and archives and that will also be part of their collections in the future. The popular belief that a decrease of 5 °C doubles the permanence of paper remains valid as long as the E_a is close to 95 kJ mol^{-1}. The permanence increases with E_a, for instance by up to 2.6 times for E_a of 130 kJ mol^{-1}. In particular, alkaline buffered paper is extremely durable and hence a reliable information carrier and art medium, especially in protected and environmentally controlled infrastructures. The environmental control for the preservation of these papers in archival contexts can be minimal due their intrinsic durability, as opposed to acidic papers with a low E_a which would significantly benefit from small climate adjustments. The isoperm approach can provide a reasonable estimate of the rate of aging of paper and can help inform decisions related to their preservation.

The results of the simulations also confirm the importance of storing mechanical pulp papers in a dry and cold environment for optimal preservation and extension of their usability to more than 500 years.

Acknowledgements
The authors would like to dedicate this paper to our late friend Luc Bourbonnais. We have played with some equations together. The authors are grateful to Valérie Dupont for her insightful contribution during the editing of this article.

Authors contributions (CRediT)
JT & ALD: Conceptualization, Methodology, Validation, Formal Analysis, Investigation, Resources, Writing - Original Draft, Visualization, Supervision, Project administration; DV, PB & SPL: Validation, Formal Analysis, Investigation, Resources.

Funding
The authors received no financial support for the research, authorship, and/or publication of this article.

Competing interests
The authors declare that no funds, grants, or other support were received during the preparation of this manuscript and that they have no relevant financial or nonfinancial interests to disclose.

References

Barański A, Dziembaj R, Konieczna-Mlenda A et al (2004) On the applicability of Arrhenius equation to accelerated tests. The case of alum-impregnated cellulose. Pol J of Chem Technol 6:1-8

Barrow WJ, Sproull RC (1959) Permanence in book papers. Science 129:1075-1084

Barrow WJ (1974) Permanence/durability of the book-VII. Physical and chemical properties of book papers, 1507 – 1949, Barrow Research Lab, Richmond

Bégin P, Deschâtelets S, Grattan D, Gurnagul N, Iraci J, Kaminska,E, Zou X (1998) The impact of lignin on paper permanence. Restaurator 19:135-154. https://doi.org/10.1515/rest.1998.19.3.135

Bigourdan J-L, Adelstein PZ, Reilly JM (1996) Acetic acid and paper alkaline reserve: assessment of a practical situation in film preservation. In Bridgland J (ed) ICOM Committee for Conservation 11th Triennial Meeting Edinburgh 1-6 September 1996. James & James, London, pp 573-579

Bogaard J, Whitmore PM (2002) Explorations of the role of humidity fluctuations in the deterioration of paper. Stud in Conserv 47(Suppl 3):11-15. https://doi.org/10.1179/sic.2002.47.s3.003

Bown R (1996) Physical and chemical aspects of the use of fillers in paper. In: Roberts, J.C. (eds) Paper Chemistry. Springer, Dordrecht, pp 195-230. https://doi.org/10.1007/978-94-011-0605-4_11

Calvini P (2005) The influence of levelling-off degree of polymerisation on the kinetics of cellulose degradation. Cellulose 12:445-447. https://doi.org/10.1007/s10570-005-2206-z

Calvini P, Gorassini A, Merlani AL (2008) On the kinetics of cellulose degradation: looking beyond the pseudo zero order rate equation. Cellulose 15:193–203

Clapp VW (1972) The story of permanent/durable book paper, 1115-1970. Restaurator 1(s3):1-51. https://doi.org/10.1515/rest.1972.1.s3.1

Ding HZ, Wang ZD (2008) On the degradation evolution equations of cellulose. Cellulose 15:205-224. https://doi.org/10.1007/s10570-007-9166-4

Du Plooy ABJ (1981) The influence of moisture content and temperature on the aging rate of paper. Appita J 34:287-292

Dupont A-L, Réau D, Bégin P, Paris-Lacombe S, Tétreault J, Mortha G (2018) Accurate molar masses of cellulose for the determination of degradation rates in complex paper samples. Carbohydr Polym 202:172-185. https://doi.org/10.1016/j.carbpol.2018.08.134

Ekenstam AA (1936) Über das verhalten der cellulose in mineralsäure-lösungen, II. mitteil: Kinetisches studium des abbaus der cellulose in säure-lösungen. Ber Dtsch Chem Ges 69:549-552

Erhardt D (1989) Relationship of reaction rates to temperature. Abbey Newsl 13:38-39

Forchheim D, Hornung U, Kruse A, Sutter T (2014) Kinetic modelling of hydrothermal lignin depolymerisation. Waste Biomass Valor (2014) 5:985-994. https://doi.org/10.1007/s12649-014-9307-6

Gray GG (1978) Determination and significance of activation energy in permanence tests. In: Williams JC (ed) Preservation of Paper and Textiles of Historic and Artistic Value, Advances in Chemistry 164, pp 286-313

Hansen BV, Vest M (2008) Lifetime of acid paper in the collection of the Royal Library. In: Strlič M and Kolar J Durability of paper and writing 2: 2nd International Symposium and Workshops, Ljubljana, Slovenia, July 7-9, 2008. Faculty of Chemistry and Chemical Technology, Ljubljana, pp 38-39

Hubbe MA, Smith RD, Zou X, Katuscak S, Potthast A, Ahn K (2017) Deacidification of acidic books and paper by means of non-aqueous dispersions of alkaline particles: A review focusing on completeness of the reaction. BioResources 12(2): 4410-4477. https://dot.org/10.15376/biores.12.2.Hubbe

Jablonsky M, Šima J, Lelovsky M (2020) Considerations on factors influencing the degradation of cellulose in alum-rosin sized paper. Carbohydrate Polymers. https://doi.org/10.1016/j.carbpol.2020.116534

Jeong M-J, Potthast A (2021) Improving the accuracy of estimating paper permanence for accelerated degradation in closed vials. Cellulose 28:4053-4068. https://doi.org/10.1007/s10570-021-03804-y

Kaminska EM, Bégin P, Grattan DW et al (2001) ASTM/ISR research program on the effects of aging on printing and writing papers: accelerated aging test method development: final report. CCI report no.70664. Canadian Conservation Institute, Ottawa

Kuhn W (1930) Über die Kinetik des Abbaues hochmolekularer Ketten. Ber Dtsch Chem Ges 63:1503-1509

Liu Y, Cigić IK, Strlič M (2017) Kinetics of accelerated degradation of historic iron gall ink-containing paper. Polym Degrad Stab 142:255-262. https://doi.org/10.1016/j.polymdegradstab.2017.07.010

Menart E, De Bruin G, Strlič M (2011), Dose-response functions for historic paper. Polym Degrad Stab 96:2029-2039. https://doi.org/10.1016/j.polymdegradstab.2011.09.002

Mochizuki Y, Itsumura H, Enomae T (2020) Mechanism of acidification that progresses in library collections of books made of alkaline paper. Restaurator 41:153-172. https://doi.org/10.1515/res-2020-0008

Parker ME, Bronlund JE, Mawson AJ (2006) Moisture sorption isotherms for paper and paperboard in food chain conditions. Packag Technol Sci 19:193-209. https://doi.org/10.1002/pts.719

Parsa Sadr A, Bosco E, Suiker ASJ (2022) Multi-scale model for time-dependent degradation of historic paper artifacts. Int J of Solids and Structures. https://doi.org/10.1016/j.ijsolstr.2022.111609

Porck, HJ (2000) Rate of paper degradation: The predictive value of artificial aging tests. European Commission on Preservation and Access, Amsterdam

Rouchon V, Belhadj O, Duranton M, Gimat A, Massiani P (2016) Application of Arrhenius law to DP and zero-span tensile strength measurements taken on iron gall ink impregnated papers: Relevance of artificial ageing protocols. Appl Phys A. https://doi.org/10.1007/s00339-016-0307-1

Sebera DK (1994) Isoperms: an environmental management tool https://cool.culturalheritage.org/byauth/sebera/isoperm/ Accessed 11 April 2023

Shahani CJ, Hengemihle FH, Weberg N (1995) The effect of fluctuations in relative humidity on library and archival materials and their aging within contained microenvironments. In Arnoult JM (ed) Proceedings of Pan-African conference on the preservation and conservation of library and archival materials. IFLA, The Hague, pp 61-70

Sharples A (1971) Acid hydrolysis and alcoholysis. In: Bikales NM, Segal L (eds) Cellulose and cellulose derivatives, Wiley-Interscience, New York, pp 991-1006

Strang T, Grattan D (2009) Temperature and humidity considerations for the preservation of organic collections - The isoperm revisited. e-PS 6:122-128

Strlič M, Grossi CM, Dillon C et al (2015) Damage function for historic paper. Part III: Isochrones and demography of collections. Herit Sci. https://doi.org/10.1186/s40494-015-0069-7

Tétreault J, Dupont A-L, Begin P, Paris S (2013) The impact of carbonyl and hydrogen peroxide vapours on cellulose degradation under ambient hygrothermal conditions. Polym Degrad Stab 98:1827–1837. https://doi.org/10.1016/j.polymdegradstab.2013.05.017

Tétreault J, Bégin P, Paris SJ, Dupont A-L (2019) Modelling considerations for the degradation of cellulosic. Cellulose 26:2013-2033. https://doi.org/10.1007/s10570-018-2156-x

Timmermann EO (2003) Multilayer sorption parameters: BET or GAB values? Colloid Surf A 220(1):235-260. https://doi.org/10.1016/S0927-7757(03)00059-1

Vibert C, Fayolle B, Ricard D, Dupont A-L (2023) Decoupling hydrolysis and oxidation of cellulose in permanent paper aged under atmospheric conditions. Carbohydr Polym. https://doi.org/10.1016/j.carbpol.2023.120727

Wilson WK, Harvey JL, Mandel JM, Worksman T (1955) Accelerating aging of records papers compared with natural aging. Tappi J 38:543-547

Young RA (1994) Comparison of the properties of chemical cellulose pulps. Cellulose 1:107-130. https://doi.org/10.1007/BF00819662

Zervos S (2010) Natural and accelerated ageing of cellulose and paper: A literature review. In: Lejeune, A, Deprez, T (eds) Cellulose: Structure and properties, derivatives and industrial uses. Nova Publishing, New York, pp 155-203

Zhang B, Huang H-J, Ramaswamy S (2008) Reaction kinetics of the hydrothermal treatment of lignin. Appl Biochem Biotechnol (2008) 147:119-131. https://doi.org/10.1007/s12010-007-8070-6

Zou X, Uesaka T, Gurnagul N (1996a) Prediction of paper permanence by accelerating aging part I. Kinetic analysis of the aging process. Cellulose 3:243-267. https://doi.org/10.1007/BF02228805

Zou X, Uesaka T, Gurnagul N (1996b) Prediction of paper permanence by accelerating aging part II. Comparison of the predictions with natural aging results. Cellulose 3:269-279. https://doi.org/10.1007/BF02228806